DOI: 10.1021/ma901246y

Macromolecules
ARTICLE

Out-of-Plane Longitudinal Elastic Modulus of Supported Polymer Thin Films

N. Gomopoulos,[†] W. Cheng,[†] M. Efremov,[‡] P. F. Nealey,[‡] and G. Fytas*[,†,§]

[†]*Max Planck Institute for Polymer Research Ackermannweg 10, 55128 Mainz, Germany,* [‡]*Department of Chemical and Biological Engineering, University of Wisconsin—Madison, Madison, Wisconsin 53706, and* [§]*Department of Materials Science, University of Crete and F.O.R.T.H., 77110 Heraklion, Greece*

Received June 10, 2009; Revised Manuscript Received July 23, 2009

ABSTRACT: We employ Brillouin light scattering to measure the longitudinal modulus in supported thin polymer films in the direction normal to the film surface. In this first systematic experimental investigation, a reflection scattering geometry was utilized to probe elastic excitations localized between the free surface and the glass substrate, thus providing a direct access to the elastic constant along this direction. Thin supported polystyrene and poly(methyl methacrylate) films with thickness in the range of 40 nm−3 μm were explored. Comparison with the in-plane elastic constant obtained from the same optical technique but in transmission scattering geometry [*Macromolecules* **2007**, *40*, 7283] revealed no prominent directional tendency of the elastic properties with thickness. Nevertheless, there is now an experimental tool to address direction-dependent elastic constants in supported thin films.

Introduction

Characterization of the mechanical properties of supported polymer films is of the key importance in advancing of the microlithography and other coating-based technologies. The demand for qualitative and nondestructive probes drives the emerging field of photoacoustic methods. Spontaneous Brillouin laser light scattering (BLS), impulsive stimulated thermal scattering (ISTS), and similar techniques are based on optical measurements of either spontaneous or laser-stimulated acoustic waves in the sample.[1−5] This approach provides fast, reliable, noncontact, and localized evaluation of elastic moduli of coatings without often challenging preparation of individually designed test specimens.[1,6] Directional selectivity of photoacoustic methods is of specific interest to the thin film mechanics as many coatings exhibit substantial anisotropy of structure and properties. Recently we have demonstrated the utility of BLS to probe the in-plane longitudinal and shear moduli in submicrometer-thick polymer films supported by a transparent substrate.[7] ISTS has been used as an alternative method for thicker films.[1] However, these experiments provide only indirect information on the out-of-plane elasticity, as studied acoustic excitations are characterized by finite in-plane wavevector components $q_{\parallel}$.[8] Direct access to the out-of-plane elastic constants implies probing of acoustic waves with wavevectors $q_{\perp}$ normal to the film surface. This measurement has been done by BLS for thick polymer films of a particular orientation relative to the incident laser beam.[9] A single mode acoustic excitation, characteristic of the effective bulk medium, has been observed.

Out-of-plane standing acoustic wave excitations in free-standing films have been known for decades.[10,11] However, the same phenomenon in supported films has been reported only recently[12] and attracts growing attention.[13−19] In this regime, computation of the elastic moduli requires only two unambiguous parameters: film thickness and mass density. Backscattering geometry is typically utilized in all these experiments: the probing laser beam hits the coating side of the sample, and the scattered light is monitored backward. However, in this case the corresponding wavevector has nonzero in-plane component $q_{\parallel}$, which complicates the spectra interpretation due to the in-plane excitations. The present scattering geometry (or refection mode) is the most appropriate for investigation of out-of-plane excitations because there is no in-plane wavevector $q_{\parallel}$ transfer. So far, forward scattering arrangement is utilized only for the Raman spectrometry setup, which has limited spectral resolution, thus restricting the thickness of testing coatings down to a few tens of nanometers.[14]

Here, we introduce the reflection-mode BLS to observe standing elastic waves in the direction perpendicular to the film surface, providing a direct way of measuring the out-of-plane elastic longitudinal modulus of thin polymer coatings. We demonstrate the utility of the method for polystyrene (PS) and poly(methyl methacrylate) (PMMA) layers with wide thickness range from 40 nm to 3 μm on a glass substrate. We have intentionally chosen these two model polymer systems on the account of the known mechanical properties in bulk and in thin films parallel to the surface.[7] Thus, BLS becomes a versatile method to measure the elastic properties of thin supported polymer films both in-plane and normal to the surface.

Experimental Section

Samples. Atactic polystyrene (PS) with molecular weight $M_w = 61.8$ kg/mol and polydispersity $M_w/M_n = 1.03$ and poly(methyl methacrylate) (PMMA), >79% syndiotactic, with $M_w = 62.5$ kg/mol and $M_w/M_n = 1.04$ were used in this work. Supported PS and PMMA films with thickness in the range 40 nm−2.8 μm were fabricated by spin-coating of 25 mm diameter microscope cover slides made of optical borosilicate glass. Solutions of polymers in toluene were used for spin-coating. The preparation and characterization of the samples have been discussed in detail elsewhere.[7]

Brillouin Light Scattering (BLS). The BLS setup used in this study is similar to the tool described in our earlier publications,[5] with the exception of the reflection scattering geometry, introduced

*To whom correspondence should be addressed.

 Published on Web 07/31/2009

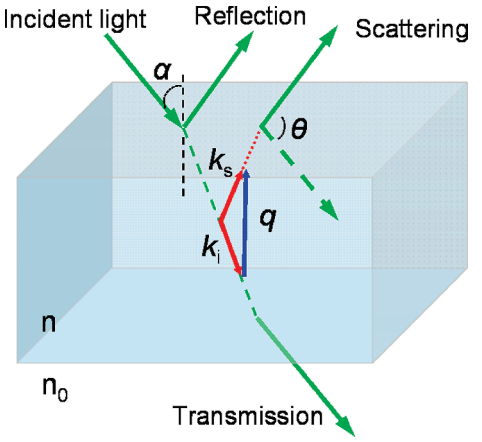

Figure 1. Reflection scattering geometry. Optical path of the incident and scattered light in a film with refractive index n and scattering angle $\theta = \pi - 2\alpha$ where α is the angle of incidence.

here. The system employs a green ($\lambda = 532$ nm) Nd:YAG laser, a precision goniometer (±0.05°), and a high-resolution six-pass tandem Fabry−Perot interferometer. Brillouin spectra (intensity of inelastically scattered light as a function of Brillouin frequency shift f) were recorded at hypersonic frequencies $f = 1-100$ GHz. Spectra are characterized by a scattering wavevector q of the corresponding propagating phonon excitation. Wavevector q is fixed for each spectrum and depends on the scattering geometry. Spectral modes relate to acoustic waves with phase velocities $v = 2\pi f/q$. Corresponding elastic moduli can be computed as $c = \rho v^2$, where ρ is the mass density.

In contrast to the typically used backscattering arrangement, reflection geometry implies that both light source and detector are located on the same side relative to the sample plane. Additionally, as shown in Figure 1, monitored scattered light is codirectional to the reflected light:

$$\theta = \pi - 2\alpha \tag{1}$$

where θ is the scattering angle and α is the incident angle. Condition (1) means that the scattering wavevector q is normal to the surface of the film: $q = q_\perp$, thus probing out-of-plane phonon excitations only.

For the reflection geometry, the range of accessible q is relatively small. A goniometer implemented in the setup allows access to θ in the range of 60°−150° (which corresponds to α in the range of 60°−15°). Simple geometric considerations give

$$q = \frac{4\pi}{\lambda}\sqrt{n^2 - \sin^2\alpha} \tag{2}$$

where n is the index of refraction of the sample material at λ wavelength. Equation 2 assumes that the index of refraction for air is 1. Using $n = 1.59$ for PS and $n = 1.50$ for PMMA,[20] eq 2 yields accessible q in the range of 0.03−0.04 nm^{-1} (approximately).

Results and Discussion

Figure 2 displays BLS spectra of supported PS films with thickness between 40 nm and 2.8 μm at $q_\perp = 0.037$ nm^{-1} and 20 °C. Since the light scattering from supported films on transparent substrates arises mainly from the elasto-optic effect,[7] reduction in the scattering volume results to an increase of acquisition times. Thus, the spectra acquisition time ranges between 1 h (for the thicker films) and about 8 h for the thinnest one. Most of the curves have remarkable multimodal shape. The thickest (2.8 μm thick) film spectrum is unimodal; the single mode corresponds to the longitudinal acoustic (LA) excitation propagating in the normal direction to the film plane. However, as film thickness decreases, the LA mode broadens and finally splits into the set of equidistant submodes.

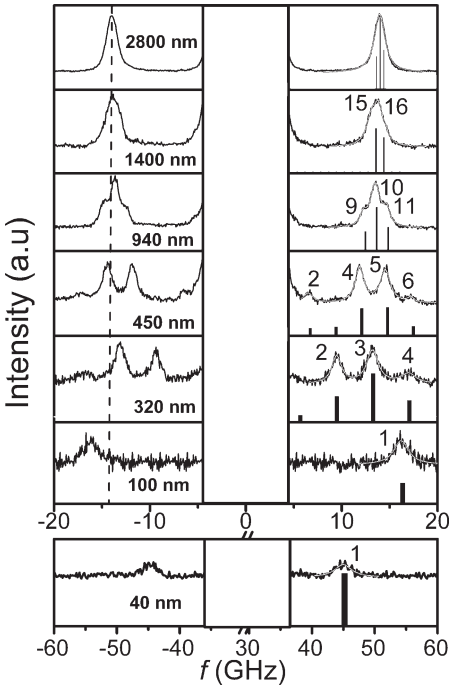

Figure 2. Normalized BLS spectra recorded at $q_\perp = 0.037$ nm^{-1} and 20 °C for a series of supported PS films with different thicknesses as indicated. Left panel: the vertical dash line represents the frequency position of the longitudinal acoustic (LA) phonon at $q_\perp = 0.037$ nm^{-1}. Right panel: red lines represent Lorentzian fits; vertical bars denote the theoretical prediction for the relative contribution of the individual modes; mode orders are indicated.

The LA mode broadening and the fine structure of BLS spectra in thin films have well-known nature.[10,11] Propagating through a thin film, a single LA phonon is localized within the distance d from the film surface, where d is the film thickness. Because of the uncertainty principle, the phonon momentum forms $\Delta p \approx h/d$ wide distribution around the mean value $\hbar q$ (here h and $\hbar$ are the Planck and reduced Planck constants, respectively). In the other terms, the wavevector q is not a certain value determined by eq 2 anymore, but has a distribution $\Delta q \approx 2\pi/d$, and the Brillouin peak has a width $\Delta f \approx v/d$.

Multiple reflections of an acoustic excitation from the film surface and interface can form *a standing wave*. First of all, it should be noted that substantial contrast of the acoustic impedance ($Z = \rho v$) between the polymer film and the substrate is the necessary condition for standing wave observation.[14] Multiphase systems with small Z mismatch between phases do not support phonon localization and exhibit an effective medium behavior.[21] The Z contrast for the samples under investigation can be defined as $\Delta Z = Z_{glass}/Z_{polymer} - 1$ and computed using mass densities and sound velocities given elsewhere.[7,20] ΔZ is equal to 5.0 for PS samples and 4.1 for PMMA samples, which are sufficient for pronounced standing wave effect.[14]

The constructive interference (CI) of the excitations gives the existence criterion for a standing wave of the order m:

$$q_m d = \pi m + \frac{\pi}{2} \tag{3}$$

where m is an integer and $\pi/2$ term is the phase shift due to the reflections on film boundaries.

Considerable range of q appeared due to the uncertainty principle makes the observation of standing waves possible.

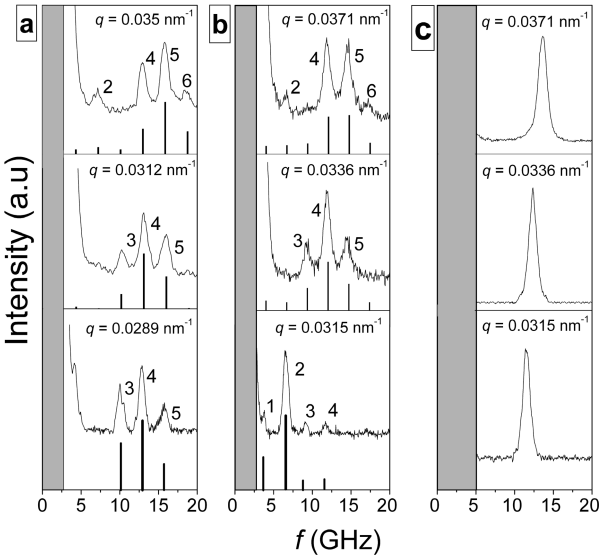

Figure 3. BLS spectra (anti-Stokes side) for (a) 490 nm thick PMMA film, (b) 450 nm thick PS film, and (c) 2800 nm thick PS film, at three different q (scattering angles 150°, 90°, and 60° from the top) and 20 °C. Solid lines represent predictions of eq 5b, and the numbers denote the order of the resolved modes.

These submodes occupy the envelope of the broadened LA phonon mode, forming the fine structure with equal interval Δf_m between peaks given by the formula directly obtained from eq 3:

$$\Delta f_m = v/2d \tag{4}$$

More rigorously, the fine structure of the BLS spectra for a supported film can be described following similar considerations in the literature.[10,11] For a nonabsorbing film/substrate system, the light scattered at angle θ has a discrete spectrum with intensity $P_s(\theta)$ given by

$$P_s(\theta) \propto \sum_m \operatorname{sinc}^2\left(q(\theta)\frac{d}{2} - (2m+1)\frac{\pi}{4}\right) \tag{5a}$$

where the mth term under the sum sign corresponds to the scattering with Brillouin shift $f_m = (2m + 1)(v/4d)$, wavevector $q(\theta)$ is defined by the system geometry (eq 1), and sinc is the cardinal sine function $\operatorname{sinc}(x) = \sin(x)/x$. In the form of the frequency shift function

$$P_s(\theta) \propto \sum_m \operatorname{sinc}^2\left[\frac{\pi d}{v}\left(q(\theta)\frac{v}{2\pi} - f_m\right)\right] \tag{5b}$$

Equation 5b demonstrates that standing wave modes f_m are localized in the $\operatorname{sinc}^2(x)$ envelope around the LA mode with shift $q(\theta)(v/2\pi)$, and the $\pi d/v$ coefficient determines the width of the envelope. Figure 2 clearly demonstrates very good agreement between the experimental and model spectra, concerning not only the eigenfrequencies but also the relative contribution of the individual modes to the BLS spectrum, notably with no adjustable parameter. The longitudinal sound velocity in PS v = 2350 m/s and d for the samples under investigation are given elsewhere.[7] Further verification of the model is performed by recording of BLS spectra at different $q_\perp$ values (see Figure 3). For the thickest sample (Figure 3c), the single LA phonon mode shifts with q change according to the relation $f = qv/2\pi$. For the films with resolved fine structure, we see the analogue: the shift of $\operatorname{sinc}^2(x)$ envelope according to the same relation. However, the

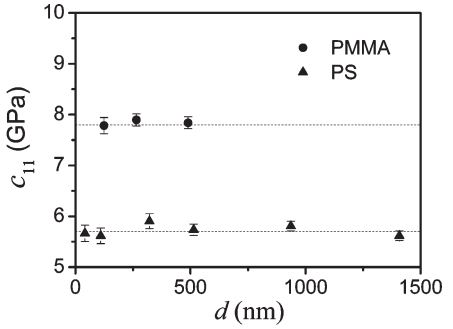

Figure 4. Longitudinal modulus in the direction normal to the film surface as a function of thickness. Solid circles correspond to PMMA and solid triangles to PS. Dash lines indicate the bulk value in each material for in-plane propagation.

Brillouin shift of the standing wave submodes does not depend on q, in accord with the constructive interference criterion. Again, Figure 3 demonstrates excellent match of experimental spectra and the function calculated by eq 5b.

The practical importance of the fine structure observation relies to the fact that computing of the elastic modulus from the Δf_m interval requires fewer parameters than using LA Brillouin shift f_{LA}. Side-by-side comparison of the longitudinal modulus c_{11} calculation methods gives

$$c_{11} = 4\rho d^2(\Delta f_m)^2 \tag{6a}$$

and

$$c_{11} = \rho\frac{\lambda^2 f_{LA}^2}{4(n^2 - \sin^2\alpha)} \tag{6b}$$

Expression 6b contains mass density and three additional parameters. Among these parameters, the refractive index n is usually considered as the main source of errors, especially for anisotropic samples.[22−25] In contrast, the method based on eq 6a requires (besides density) film thickness value only, which can be measured by a number of methods with adequate accuracy.

Nevertheless, as expected, both formulas 6a and 6b give the same result if the parameters of the equations are correct. This comparison presents additional possibility to verify our interpretation of the experimental data obtained by the BLS setup with reflection geometry. Indeed, for isotropic films like PS and PMMA coatings studied here, in-plane modulus c_{11} obtained earlier by backscattering geometry[6] using equation similar to eq 6b precisely agrees with the out-of-plane c_{11} modulus calculated by eq 6a. Figure 4 demonstrates this agreement. It also shows that the elastic modulus does not depend on thickness for films in the range from bulk samples down to 40 nm thick coatings. While this mechanical isotropy might be expected for these systems of Figure 4, its first experimental verification for thin films constitutes a significant knowledge concerning chain confinement.

It is worth to note that observation of the fine structure is limited for thick (micrometers) films by instrumental resolution factor. The computed spacing between adjacent standing wave modes Δf is plotted as a function of PS film thickness, d, in Figure 5 along with the experimental values (given in Figure 2). As shown, for a typical instrumental resolution of about 0.25 GHz, localized modes can, in principle, be resolved for films up to about 4 μm thick. However, in the experiment, the fine structure is consistently resolved for PS films as thick as 1.4 μm only (Figure 5b). A PS film with $d = 2.8$ μm, i.e., $qd \gg 1$, exhibits a pure LA phonon (Figure 3c) that displays the expected linear dispersion (inset to Figure 5a).

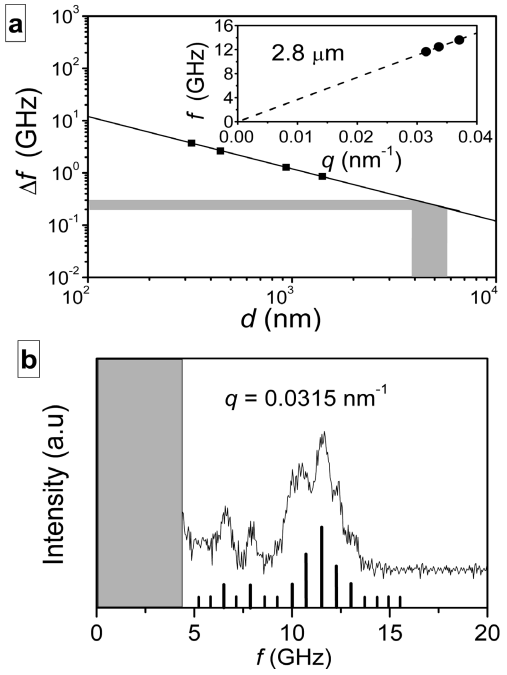

Figure 5. (a) Frequency spacing between adjacent localized modes plotted vs film thickness. The solid points and the solid line represent the experimental (Figure 2) and computed values, respectively. The shaded area indicates the upper thickness limit (~4 μm) for an instrumental resolution of about 0.25 GHz. Inset: the acoustic behavior of the longitudinal acoustic mode in a thick (2.8 μm) PS film. (b) Resolved standing wave modes for a 1.4 μm thick PS film, $q = 0.0315$ nm^{-1} ($\theta = 60°$). Solid lines represent predictions of eq 5b.

Concluding Remarks

In summary, spontaneous Brillouin light scattering spectroscopy is a powerful tool for nondestructive and direction-dependent measurements of elastic moduli in supported polymer films of micrometer and submicrometer thickness. The reflection geometry of the BLS experimental setup, introduced here, is the adequate method for probing out-of-plane elastic properties exclusively. The fine structure revealed in Brillouin spectra for submicrometer PS and PMMA films on a glass substrate provides advanced method of computing the out-of-plane elastic constants. This method requires only two additional parameters for modulus calculation: mass density and film thickness, which can be measured with sufficient precision by other methods. Excellent agreement between the out-of-plane elastic moduli obtained by the reported technique and the in-plane moduli measured by typical backscattering geometry setup is observed. The agreement verifies the consistency of the method and also supports the in-plane/out-of-plane isotropy of the studied polymer films in a wide thickness range.

Acknowledgment. M.E. and P.F.N. thank the Global Research Corporation (Grants 2005-OCHH-985 and 2008-OCHH-164) and the National Science Foundation Nanoscale Science and Engineering Center at the University of Wisconsin—Madison (Grant DMR0425880) for the support.

References and Notes

(1) Rogers, J. A.; Maznev, A. A.; Banet, M. J.; Nelson, K. A. *Annu. Rev. Mater. Sci.* **2000**, *30*, 117.
(2) Hillebrands, B.; Lee, S.; Stegeman, G. I. *Phys. Rev. Lett.* **1988**, *60*, 832.
(3) Forrest, J. A.; Dalnoki-Veress, K.; Stevens, J. R.; Dutcher, J. R. *Phys. Rev. Lett.* **1996**, *77*, 2002.
(4) Hartschuh, R.; Ding, Y.; Roh, J. H.; Kisliuk, A.; Sokolov, A. P.; Soles, C. L.; Jones, R. L.; Hu, T. J.; Wu, W. L.; Mahorowala, A. P. *J. Polym. Sci., Part B: Polym. Phys.* **2004**, *42*, 1106–1113.
(5) Penciu, R. S.; Kriegs, H.; Petekidis, G.; Fytas, G.; Economou, E. N. *J. Chem. Phys.* **2003**, *118*, 5224.
(6) Hemker, K. J.; Sharpe, W. N. Jr. *Annu. Rev. Mater. Res.* **2007**, *37*, 93–126.
(7) Cheng, W.; Sainidou, R.; Burgardt, P.; Stefanou, N.; Kiyanova, A.; Efremov, M.; Fytas, G.; Nealey, P. F. *Macromolecules* **2007**, *40*, 7283–7290.
(8) Rogers, J. A.; Dhar, L.; Nelson, K. A. *Appl. Phys. Lett.* **1994**, *65*, 312–314.
(9) Cheng, W.; Gorishnyy, T.; Krikorian, V.; Fytas, G.; Thomas, E. L. *Macromolecules* **2006**, *39*, 9614–9620.
(10) Sandercock, J. R. *Phys. Rev. Lett.* **1972**, *28*, 237.
(11) Sandercock, J. R. *Phys. Rev. Lett.* **1972**, *29*, 1735.
(12) Zhang, X.; Sooryakumar, R.; Every, A. G.; Manghnani, M. H. *Phys. Rev. B* **2001**, *64*, 081402.
(13) Zhang, X.; Bandhu, R. S.; Sooryakumar, R.; Jonker, B. T. *Phys. Rev. B* **2003**, *67*, 075407.
(14) Groenen, J.; Poinsotte, F.; Zwick, A.; Torres, C. M. S.; Prunnila, M.; Ahopelto, J. *Phys. Rev. B* **2008**, *77*, 045420.
(15) Nakamura, N.; Ogi, H.; Hirao, M. *Phys. Rev. B* **2008**, *77*, 245416.
(16) Link, A.; Sooryakumar, R.; Bandhu, R. S.; Antonelli, G. A. *J. Appl. Phys.* **2006**, *100*, 013507.
(17) Bandhu, R. S.; Zhang, X.; Sooryakumar, R.; Bussmann, K. *Phys. Rev. B* **2004**, *70*, 075409.
(18) Mathe, B. A.; Comins, J. D.; Every, A. G. *J. Phys.: Conf. Ser.* **2007**, *92*, 012096.
(19) Ogi, H.; Shagawa, T.; Nakamura, N.; Hirao, M.; Odaka, H.; Kihara, N. *Phys. Rev. B* **2008**, *78*, 134204.
(20) Mark, J. E., Ed. *Physical Properties of Polymers Handbook*; Springer: New York, 2007.
(21) Cheng, W.; Gomopoulos, N.; Fytas, G.; Gorishnyy, T. J.; Walish, J.; Thomas, E. L.; Hiltner, A.; Baer, E. *Nano Lett.* **2008**, *8*, 1423–1428.
(22) Van Workum, K.; de Pablo, J. J. *Nano Lett.* **2003**, *3*, 1405–1410.
(23) Yoshimoto, K.; Tushar, S. J.; Van Workun, K.; Nealey, P. F.; De Pablo, J. J. *Phys. Rev. Lett.* **2004**, *93*, 175501.
(24) Varnik, F.; Baschnagel, J.; Binder, K. *J. Chem. Phys.* **2000**, *113*, 4444.
(25) Lee, J. Y.; Su, K. E.; Chan, E. P.; Zhang, Q.; Emrick, T.; Crosby, A. J. *Macromolecules* **2007**, *40*, 7755.